

EXACT CONTROLLABILITY AND DOMAIN DECOMPOSITION
METHODS WITH NON-MATCHING GRIDS FOR
THE COMPUTATION OF SCATTERING WAVES

M.O. BRISTEAU, E.J. DEAN, R. GLOWINSKI, V. KWOK, J. PERIAUX

ABSTRACT. The main goal of this article is to discuss the solution of scattering problems for coated obstacles by a methodology combining exact controllability techniques and domain decomposition algorithms. In this article, domain decomposition techniques are used to split the computational domain into smaller ones and also to take into account the different physical properties taking place in different regions, which may require the coupling of local approximate solutions defined over non-matching finite element meshes; this coupling is easily achieved through a weak formulation of the interface, using Lagrange multipliers. The results of numerical experiments for documented aerospace test cases are presented, showing the good performances of these new methods, particularly for non-convex reflectors.

1. Introduction.

In a recent publication (see [1]), the authors have introduced a novel approach for the computation of scattering waves by coated obstacles. This methodology rests on the combination of:

- (i) An *exact controllability* formulation à la *Hilbert Uniqueness Methods* (HUM, [2]), which allows the fast calculation of limit cycles for wave equations.
- (ii) *Domain decomposition* methods for non-overlapping subdomains where the interface compatibility conditions are enforced via *Lagrange multipliers*. (For wave equations this method was introduced in Reference [3], to our knowledge.)

In References [1] and [3] the domain decomposition methodology was used to decouple subregions with different physical properties, such as air and the coating material, requiring meshes which do not match at the interface if one wishes to use the same time discretization step in all subregions. In the present article, we go one step further by introducing domain decompositions whose main goal is to further split the computational domain (for distributed parallel computing purposes, for example). The resulting methodology is particularly robust and well-suited to scattering by non-convex reflectors, which is typical in industrial applications.

2. The Generalized Helmholtz Equation and its Equivalent Wave Problem.

The *Helmholtz equation* (Maxwell equations in two dimensions for the T.M. mode) for *heterogeneous media* is given by

$$(2.1) \quad \epsilon k^2 U + \nabla \cdot \mu^{-1} \nabla U = F \text{ in } \Omega,$$

where ϵ and μ are the *permittivity* and *permeability coefficients*, respectively (we assume that ϵ and μ are positive); Ω is the region of \mathbb{R}^2 where the propagation phenomenon is taking place. We suppose that Ω is *bounded* (see Figure 2.1 below) by an artificial boundary Γ , where an *absorbing boundary* condition is prescribed. For simplicity, we specify on Γ

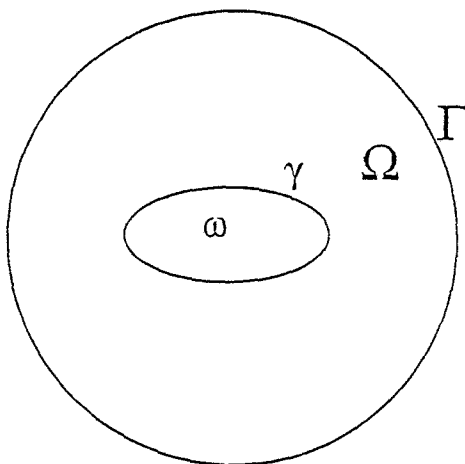


Figure 2.1

$$(2.2) \quad \frac{\partial U}{\partial n} + \sqrt{\epsilon \mu} i k U = 0,$$

to be completed by a Dirichlet condition on the boundary γ of the reflector ω , namely

$$(2.3) \quad U = G,$$

where $-G$ is the incident field at γ . All of the above functions are complex valued. The wave number k is given by

$$(2.4) \quad k = 2\pi/T,$$

T being the time period.

Remark 2.1. if Ω is "filled" with air (or void), $F = 0$ in (2.1) for incident monochromatic waves. The function U represents the scattered field. Condition (2.2) assumes that Γ is located in air (or void).

Following [4], we observe that (2.1)-(2.3) is equivalent to finding T -periodic solutions of

$$(2.5) \quad \epsilon u_{tt} - \nabla \cdot \mu^{-1} \nabla u = f \text{ in } \Omega \times (0, T) (= Q),$$

$$(2.6) \quad u = g \text{ on } \gamma \times (0, T) (= \sigma),$$

$$(2.7) \quad \frac{\partial u}{\partial n} + \sqrt{\epsilon \mu} \frac{\partial u}{\partial t} = 0 \text{ on } \Gamma \times (0, T) (= \Sigma)$$

where $u(x, t) = \text{Re}(U(x)e^{ikt})$. From the T -periodicity, u satisfies

$$(2.8) \quad u(0) = u(T), \quad u_t(0) = u_t(T).$$

3. Exact Controllability Solution Methods.

In order to solve (2.1)-(2.3) or (2.5)-(2.8) by controllability methods inspired from HUM, we observe that solving the above problems is equivalent to finding a pair $\{e_0, e_1\}$ so that

$$(3.1) \quad u(0) = e_0, u_t(0) = e_1,$$

$$(3.2) \quad u(T) = e_0, u_t(T) = e_1,$$

with u solution of (2.5)-(2.7). Problem (2.5)-(2.7), (3.1), (3.2) is an *exact controllability problem* which can be solved by methods directly inspired from the J.L. Lions *Hilbert Uniqueness Method* (HUM) (see, e.g., [2], [5], [6] for an introduction to this method and for further applications).

4. Least Squares Formulation of Problem (2.5)-(2.7), (3.1), (3.2).

In order to apply HUM to the solution of problem (2.5)-(2.7), (3.1), (3.2) an appropriate choice for the space containing $\{e_0, e_1\}$ is

$$(4.1) \quad E = V_g \times L^2(\Omega), \text{ with } V_g = \{\varphi \mid \varphi \in H^1(\Omega), \varphi|_{\gamma} = g(0)\}.$$

A least squares formulation is given by

$$(4.2) \quad \text{Min}_{v \in E} J(v)$$

with $v = \{v_0, v_1\}$ and

$$(4.3) \quad J(v) = \frac{1}{2} \int_{\Omega} [\mu^{-1} |\nabla(y(T) - v_0)|^2 + \epsilon |y_t(T) - v_1|^2] dx,$$

where, in (4.3), y is the solution of

$$(4.4) \quad \epsilon y_{tt} - \nabla \cdot \mu^{-1} \nabla y = f \text{ in } Q,$$

$$(4.5) \quad y = g \text{ on } \sigma,$$

$$(4.6) \quad \frac{\partial y}{\partial n} + \sqrt{\epsilon \mu} \frac{\partial y}{\partial t} = 0 \text{ on } \sigma,$$

$$(4.7) \quad y(0) = v_0, y_t(0) = v_1.$$

The choice of J is quite natural indeed since the total energy of the system is given by

$$\mathcal{E}(t) = \frac{1}{2} \int_{\Omega} [\epsilon |y_t(t)|^2 + \mu^{-1} |\nabla y(t)|^2] dx.$$

The least squares problem (4.2) can be solved by a *conjugate gradient algorithm* operating in space E ; such an algorithm is described in Section 6 of [1].

5. Calculation of J' .

In order to solve problem (4.2) by a conjugate gradient algorithm, we need to know the differential J' of J . To compute J' we shall use the *perturbation method* described in Section 5 of [1]. We obtain then

$$(5.1) \quad \left\{ \begin{aligned} \langle J'(\mathbf{v}), \mathbf{w} \rangle = & \int_{\Omega} \mu^{-1} \nabla(v_0 - y(T)) \cdot \nabla w_0 dx \\ & - \int_{\Omega} \epsilon p_t(0) w_0 dx + \int_{\Gamma} \sqrt{\frac{\epsilon}{\mu}} p(0) w_0 d\Gamma \\ & + \int_{\Omega} \epsilon p(0) w_1 dx + \int_{\Omega} \epsilon (v_1 - y_t(T)) w_1 dx, \end{aligned} \right.$$

for all $\mathbf{v} = \{v_0, v_1\} \in E$ and all $\mathbf{w} = \{w_0, w_1\} \in E$, with $E_0 = V_0 \times L^2(\Omega)$ and

$$V_0 = \{z \mid z \in H^1(\Omega), z = 0 \text{ on } \gamma\};$$

in (5.1), the function p is (uniquely) defined by the following adjoint system

$$(5.2) \quad \epsilon p_{tt} - \nabla \cdot \mu^{-1} \nabla p = 0 \text{ in } Q,$$

$$(5.3) \quad \frac{\partial p}{\partial n} - \sqrt{\epsilon \mu} \frac{\partial p}{\partial t} = 0 \text{ on } \sigma,$$

$$(5.4) \quad p = 0 \text{ on } \sigma,$$

$$(5.5) \quad p(T) = y_t(T) - v_1,$$

$$(5.6) \quad \begin{cases} \int_{\Omega} \epsilon p_t(T) z \, dx = \int_{\Gamma} \sqrt{\frac{\epsilon}{\mu}} (y_t(T) - v_1) z \, d\Gamma \\ - \int_{\Omega} \mu^{-1} \nabla(y(T) - v_0) \cdot \nabla z \, dx, \forall z \in V_0. \end{cases}$$

From the knowledge of J' we can solve problem (4.2) by a conjugate gradient algorithm operating in space $E = V_g \times L_2(\Omega)$. As already mentioned, such an algorithm is described in [1, Section 6]: each iteration requires the solution of *one forward wave equation* (such as (4.4)-(4.7)), of *one backward wave equation* (such as (5.2)-(5.6)), and of an *elliptic problem* in Ω , associated to the bilinear form

$$\{\varphi, \psi\} \rightarrow \int_{\Omega} \nabla \varphi \cdot \nabla \psi \, dx.$$

6. A Finite-Difference/Finite-Element Implementation.

The practical implementation of the controllability method is based upon a *time discretization* by a *centered explicit finite-difference scheme*. This scheme is combined with *piecewise-linear finite-element approximations* for the *space variables*. We use *mass lumping* through numerical integration by the *trapezoidal rule* to obtain a *diagonal mass matrix* for the acceleration terms. The fully discrete scheme has to satisfy a stability condition such as $\Delta t \leq Ch$, where C is independent of h and Δt . To obtain accurate solutions, we need to have h at least *ten times smaller* than the wavelength; consequently, Δt has to be at least ten times smaller than the period. If we assume that the number of iterations is independent of h and Δt (assumptions supported by numerical experiments), the solution of the Helmholtz equation via the new approach involves a number of operations which for a given value of k is proportional to the number of grid points; for this estimate we do not take into account the time spent at solving the elliptic problems mentioned in Section 5, which in two dimensions is negligible compared to the time required to solve the wave equations; in three dimensions it remains to see if the same conclusion holds.

Remark 6.1. In [6] and [7] one may find the detailed description of the solution method for a controllability problem for the wave equation closely related to the one discussed in this article. The problem in [6] and [7] is space and time discretized by finite-element and finite-difference methods similar to those advocated above.

7. Combining Controllability and Comain Decomposition Methods.

7.1 Generalities.

In the particular case of the scattering of waves by coated materials (see Figure 7.1 for such a situation), the waves propagate faster in the surrounding air (or void) than in the

coating. If one wishes to use the same time discretization step Δt everywhere with a *local CFL* number of the order of one, it is necessary to employ local meshes with quite different space discretization steps. This observation leads quite naturally to a *domain decomposition method* associated to the physical heterogeneities of the problem; furthermore, it leads to the use of space discretization meshes which do not match at the interface (see Figure 7.2). The crucial point when combining exact controllability and domain decomposition with non-matching finite-element meshes is to develop efficient solution methods for wave problems such as (2.5)-(2.7), (3.1) when ϵ and μ are piecewise continuous. For simplicity we shall discuss first the solution of (2.5)-(2.7), (3.1) for the physical situation associated to figure 7.1 whose notation has been kept.

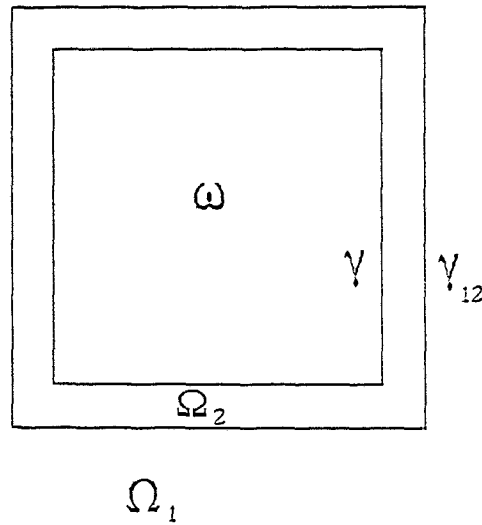


Figure 7.1

7.2 A Domain Decomposition Method for Linear Wave Problems.

The problem to be solved is described by

$$(7.1) \quad \epsilon_i \frac{\partial^2 u_i}{\partial t^2} - \nabla \cdot (\mu_i^{-1} \nabla u_i) = -\epsilon_i \frac{\partial^2 u^{inc}}{\partial t^2} \\ + \nabla \cdot (\mu_i^{-1} \nabla u^{inc}) \text{ in } Q_i = \Omega_i \times (0, T), \quad \forall i = 1, 2,$$

$$(7.2) \quad u_2 = -u^{inc} \text{ on } \sigma,$$

$$(7.3) \quad \sum_{i=1}^2 \mu_i^{-1} \frac{\partial u_i}{\partial n_i} = - \sum_{i=1}^2 \mu_i^{-1} \frac{\partial u^{inc}}{\partial n_i} \text{ on } \sigma_{12} = \gamma_{12} \times (0, T),$$

$$(7.4) \quad u_1 = u_2 \text{ on } \sigma_{12},$$

$$(7.5) \quad \frac{\partial u_1}{\partial n_1} + \sqrt{\epsilon_1 \mu_1} \frac{\partial u_1}{\partial t} = 0 \text{ on } \sigma,$$

$$(7.6) \quad u_i(0) = e_0 |_{\Omega_i}, \quad \frac{\partial u_i}{\partial t}(0) = e_1 |_{\Omega_i}, \quad \forall i = 1, 2,$$

where, in (7.1)-(7.6), u_i is the local *scattered field* and u^{inc} the *incident field*. In the case of monochromatic plane waves, the incident field has the following complex representation:

$$u^{inc}(x, t) = -e^{ik(t - \sum_{j=1}^d a_j x_j)}$$

with

$$x = \{x_j\}_{j=1}^d \quad (d = 2 \text{ or } 3)$$

and

$$a = \{a_j\}_{j=1}^d$$

satisfying

$$\sum_{j=1}^d a_j^2 = 1$$

(we assume that in air (or void) the propagation velocity is $c = 1$).

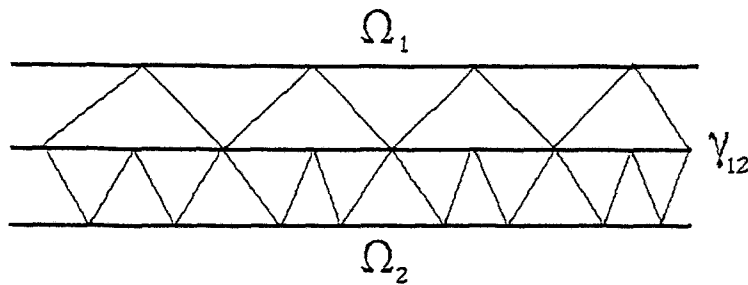


Figure 7.2

Remark 7.1. If medium $i = 1$ is either air or void, then the right-hand side of (7.1) vanishes (incidentally this right-hand side is the function f in (2.5), to be used from now on).

To solve (7.1)-(7.6) by domain decomposition, we observe (following [3]) that this system is equivalent to finding $\{u_1, u_2, \lambda\}$ so that

$$(7.7) \quad \begin{cases} \sum_{i=1}^2 \int_{\Omega_i} \epsilon_i \frac{\partial^2 u_i}{\partial t^2} v_i dx + \sum_{i=1}^2 \int_{\Omega_i} \mu_i^{-1} \nabla u_i \cdot \nabla v_i dx + \int_{\Gamma} \sqrt{\frac{\epsilon_1}{\mu_1}} \frac{\partial u_1}{\partial t} v_1 d\Gamma \\ = \int_{\gamma_{12}} \lambda (v_2 - v_1) d\gamma_{12} - \sum_{i=1}^2 \int_{\gamma_{12}} \mu_i^{-1} \frac{\partial u_i^{inc}}{\partial n_i} v_i d\gamma_{12} \\ + \sum_{i=1}^2 \int_{\Omega_i} f v_i dx, \forall \{v_1, v_2\} \in V_1 \times V_2, \end{cases}$$

$$(7.8) \quad \int_{\gamma_{12}} \mu (u_2 - u_1) d\gamma_{12} = 0, \forall \mu \in L^2(\gamma_{12}),$$

$$(7.9) \quad u_2 = g \text{ on } \sigma,$$

$$(7.10) \quad u_i(0) = e_0 |_{\Omega_i}, \frac{\partial u_i}{\partial t}(0) = e_1 |_{\Omega_i}, \forall i = 1, 2.$$

In (7.7), V_1 and V_2 are defined by

$$(7.11) \quad V_1 = H^1(\Omega_1), \quad v_2 = \{v_2 \in H^1(\Omega_2), v_2 = 0 \text{ on } \gamma\}.$$

Remark 7.2. The Lagrange multiplier treatment of matching conditions such as (7.3) and (7.4) is not new; it has been used systematically for the solution of elliptic or parabolic problems (see, e.g., [3], [8], and [9] and the references therein).

Remark 7.3. In the particular case of either air/air or coating/coating interfaces, everything which has been written previously still holds (particularly Remark 7.1); actually we have now a much simpler situation since for these two cases we can use local meshes which match at the subdomain interfaces. Such a situation will be considered in Section 8.

7.3. Time Discretization and Domain Decomposition.

In this section we shall use, for simplicity, the formalism of the continuous problem. However, the following approximation makes full sense only when V_1, V_2 , and $L^2(\gamma_{12})$ have been approximated by well-chosen finite-dimensional spaces; we shall address this issue in Section 7.4. Let $\Delta t (> 0)$ be a *time discretization step*; denoting by u^n an approximation of $u(n\Delta t)$, we approximate (7.7)-(7.10) by

$$(7.12) \quad \begin{cases} \sum_{i=1}^2 \int_{\Omega_i} \epsilon_i \frac{u_i^{n+1} + u_i^{n-1} - 2u_i^n}{|\Delta t|^2} v_i dx + \int_{\Omega_i} \mu_i^{-1} \nabla u_i^n \cdot \nabla v_i dx \\ + \int_{\Gamma} \sqrt{\frac{\epsilon_1}{\mu_1}} \frac{u_1^{n+1} - u_1^{n-1}}{2\Delta t} v_1 d\Gamma = \int_{\gamma_{12}} \lambda^n (v_2 - v_1) d\gamma_{12} \\ - \sum_{i=1}^2 \int_{\gamma_{12}} \mu_i^{-1} \frac{\partial u_i^{inc}}{\partial n_i} (n\Delta t) v_i d\gamma + \sum_{i=1}^2 \int_{\Omega_i} f^n v_i dx, \forall \{v_1, v_2\} \in V_1 \times V_2, \end{cases}$$

$$(7.13) \quad \int_{\gamma_{12}} \mu(u_2^{n+1} - u_1^{n+1})d\gamma_{12} = 0, \quad \forall \mu \in L^2(\gamma_{12}), \forall n \geq 0,$$

$$(7.14) \quad u_2^{n+1} = g^{n+1} \text{ on } \gamma,$$

$$(7.15) \quad u_i^0 = e_0 |_{\Omega_i}, u_i^1 - u_i^{-1} = 2\Delta t e_1 |_{\Omega_i}, \quad \forall i = 1, 2.$$

Combining (7.13), (7.14) will imply that relation (7.13) also holds for $n = -1$ and $n = -2$; this property is important for accuracy and stability purposes.

Remark 7.4. Scheme (7.12)-(7.15) is a domain decomposition implementation of the well-known *second-order explicit finite-differences scheme* for the wave equation.

7.4 Space/Time Discretization and Domain Decomposition.

In this section, we shall discuss a *finite-element* realization of scheme (7.12)-(7.15) and also the stability of the corresponding fully discrete scheme. We shall also discuss practicalities such as the use of *numerical integration* and the *iterative* or *direct computation* of the discrete multipliers.

7.4.1. A Fully Discrete Domain Decomposition Method.

Let W_1, W_2 , and Λ be finite-dimensional subspaces of V_1, V_2 and $L^2(\gamma_{12})$, respectively. We denote by H_{2h} the discrete equivalent of $H^1(\Omega_2)$. We approximate then (7.12)-(7.15) by

$$(7.16) \quad \left\{ \begin{array}{l} \sum_{i=1}^2 [\int_{\Omega_i} \epsilon_i \frac{u_i^{n+1} + u_i^{n-1} - 2u_i^n}{|\Delta t|^2} v_i \, dx \\ + \int_{\Omega_i} \mu_i^{-1} \nabla u_i^n \cdot \nabla v_i \, dx] + \int_{\Gamma} \sqrt{\frac{\epsilon_1}{\mu_1}} \frac{u_1^{n+1} - u_1^{n-1}}{2\Delta t} v_1 \, d\Gamma \\ = \int_{\gamma_{12}} \lambda^n (v_2 - v_1) d\gamma_{12} - \sum_{i=1}^2 \int_{\gamma_{12}} \mu_i^{-1} \frac{\partial u_i^{inc}}{\partial n_i} (n\Delta t) v_i \, d\gamma + \sum_{i=1}^2 \int_{\Omega_i} f^n v_i \, dx, \\ \forall \{v_1, v_2\} \in W_1 \times W_2; \{u_1^{n+1}, u_2^{n+2}\} \in W_1 \times H_{2h}^1, \end{array} \right.$$

$$(7.17) \quad \int_{\gamma_{12}} \mu(u_2^{n+1} - u_1^{n+1})d\gamma_{12} = 0, \quad \forall \mu \in \Lambda, \forall n \geq 0; \lambda^n \in \Lambda,$$

$$(7.18) \quad u_2^{n+1} = g_h^{n+1} \text{ on } \gamma,$$

$$(7.19) \quad u_i^0 = e_{0h} |_{\Omega_i}, u_i^1 - u_i^{-1} = 2\Delta t e_{1h} |_{\Omega_i}, \quad \forall i = 1, 2.$$

In (7.16)-(7.10), h is a space-discretization parameter and e_{0h}, e_{1h} and h_h are approximations of e_0, e_1 , and g , respectively; we suppose that e_{0h} and e_{1h} are continuous at γ_{12} (we have dropped the subscript h in (7.16)-(7.19), where u_1^j, u_2^j, λ^j are approximations of the related functions in (7.12)-(7.15)).

7.4.2. *Practical Solutions of Problems (7.16)-(7.18).*

Expanding $u_1^{n+1}, u_2^{n+1}, \lambda^n$ on vector bases of W_1, H_{2h}^1 , and Λ , we reduce the solution of problem (7.16)-(7.18) to the solution of a linear system of the following (saddle-point) type:

$$(7.20) \quad \begin{cases} Ax + B^t y = b, \\ Bx = c. \end{cases}$$

In (7.20), A is an $N \times N$ matrix, symmetric and positive definite (possibly diagonal; see [3, Section 4.1]), B is a $M \times N$ matrix (with $M \ll N$), and b and c belong to \mathbb{R}^N and \mathbb{R}^M , respectively. Problem (7.6) has a unique solution in $\mathbb{R}^N \times (\mathbb{R}^M / \ker B^t)$ if and only if c belongs to $R(B)$ (the range of B). From the fact that A is a regular matrix, we can eliminate x from (7.20); we obtain then that y is a solution of the following linear system

$$(7.21) \quad BA^{-1}B^t y = BA^{-1}b - c.$$

For the particular problem considered here, matrix $BA^{-1}B^t$ is well-conditioned (on $\mathbb{R}^M / \ker B^t$) for small values of Δt ; this property strongly suggests a *conjugate gradient* solution for problem (7.21) (and (7.20), consequently). Such an algorithm is described in, e.g., [1, Section 8.4.2], [10], [11].

7.4.3. *Further Comments.*

The domain decomposition method discussed in the above paragraphs can be generalized easily to *strip domain decompositions* like the one shown in Figure 7.2(a). In the case of *box domain decompositions*, like the one of Figure 7.2(b), crossing points (like C) require special attention as shown in [3, Section 4.3].

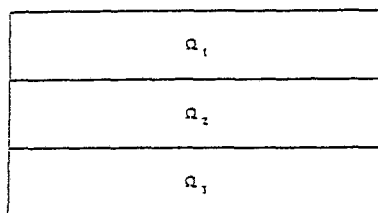


Figure 7.2(a)

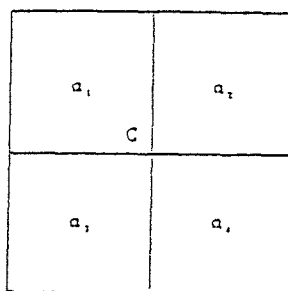


Figure 7.2(b)

8. Numerical Experiments.

The above methods have been applied to the solution of various test problems in [1, Section 9] and in [12, Chapter 4]. The test problem that we consider here concerns the scattering of a planar wave by a two-piece reflector consisting of two identical NACA 0012

airfoils whose chords are parallel; the distance between the two airfoils is λ_0 (wavelength in air); we suppose that the chords are horizontal with the leading edges on the left and that both airfoils are perfect reflectors. This two-piece reflector is illuminated by an incident planar wave coming from the upper left with a 45 degree angle of incidence. We suppose that the frequency of the incident wave is $f = 1.2$ GHz implying that the wavelength in air is $\lambda_0 = .25$ m. We suppose that the distance between the airfoils is λ_0 , that the chord length is $4\lambda_0$. We suppose next that both airfoils have been coated by a material whose relative permittivity and permeability are 7.4 and 1.4, respectively, implying that waves propagate in the coating 3.2 times slower than in air or void; the thickness of the coating is $\lambda_0/10$ in the normal direction. In order to simulate numerically the scattering of the incident wave by the above reflectors, we embed them in a rectangular domain; the distance between the boundary of the two-piece reflector and the boundary of the embedding domain has been taken equal to $3\lambda_0$. We have chosen as time step $\Delta t = T/75$, where $T = 1/f = .83 \times 10^{-9}$. The space discretization mesh is 4 times finer in the coating regions than in air. We have visualized in Figure 8.1 the four subdomain decomposition which has been used to compute the scattered field:

- (i) The two coating regions; each contains 2816 triangles and 1760 vertices; we shall denote by Ω_3 (resp. Ω_4) the upper (resp. lower) one (see lower part of the figure).
- (ii) A region denoted by Ω_2 , which closely surrounds the coated reflectors and which totally located in air (middle part of the figure); it contains 2312 triangles and 1329 reflectors.
- (iii) Finally, the "rectangular" ring (upper part of the figure) which surrounds the airfoils and the three other subdomains; it has been denoted by Ω_1 and contains 21,668 triangles and 11,130 vertices.

We have visualized on Figures 8.2 through 8.5 the contours of the scattered field in $\Omega_1, \Omega_2, \Omega_3, \Omega_4$, respectively. For further details on these numerical experiments see [12].

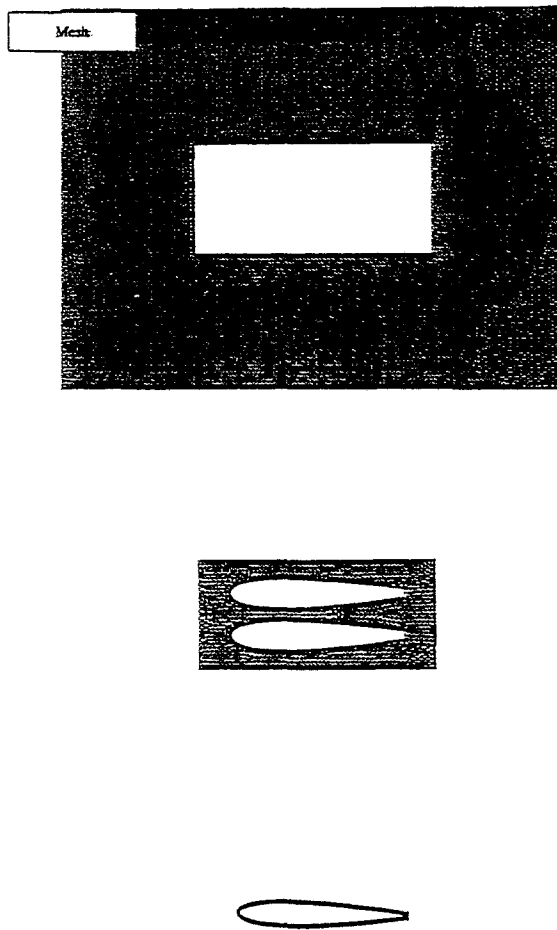


Figure 8.1: The subdomains and their finite element grid.



Figure 8.2

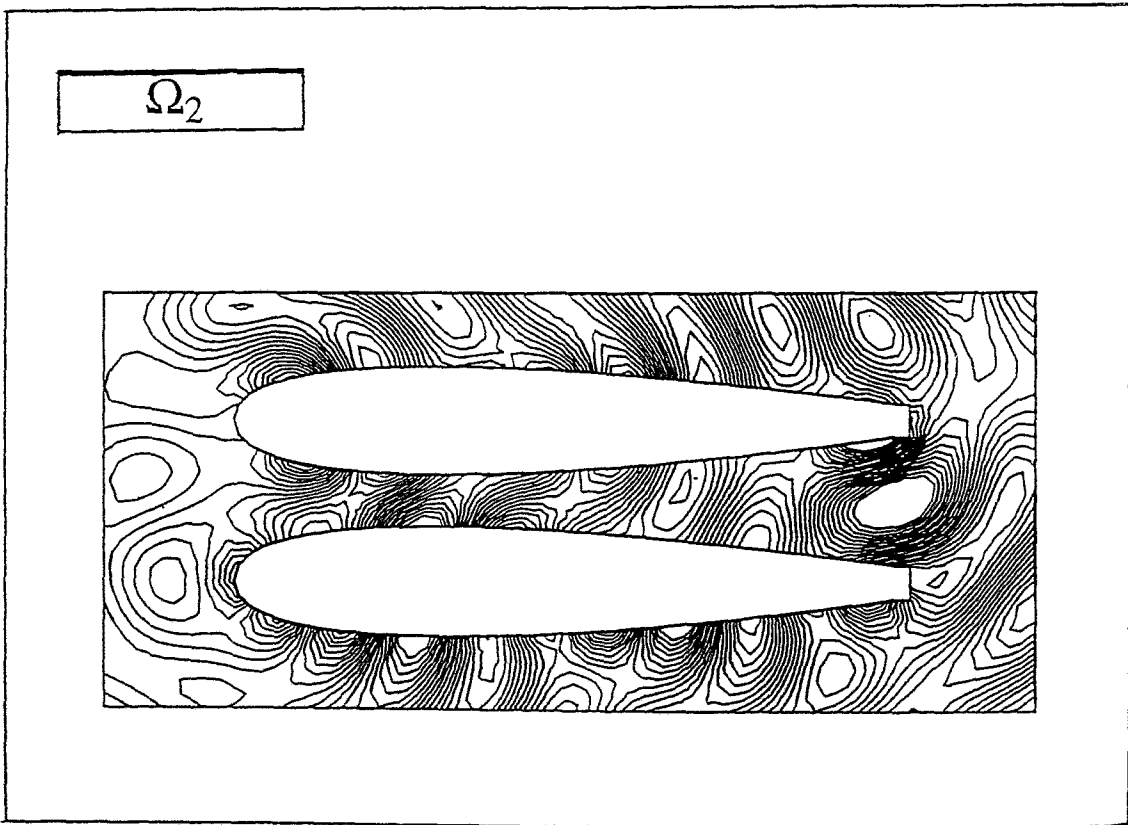


Figure 8.3

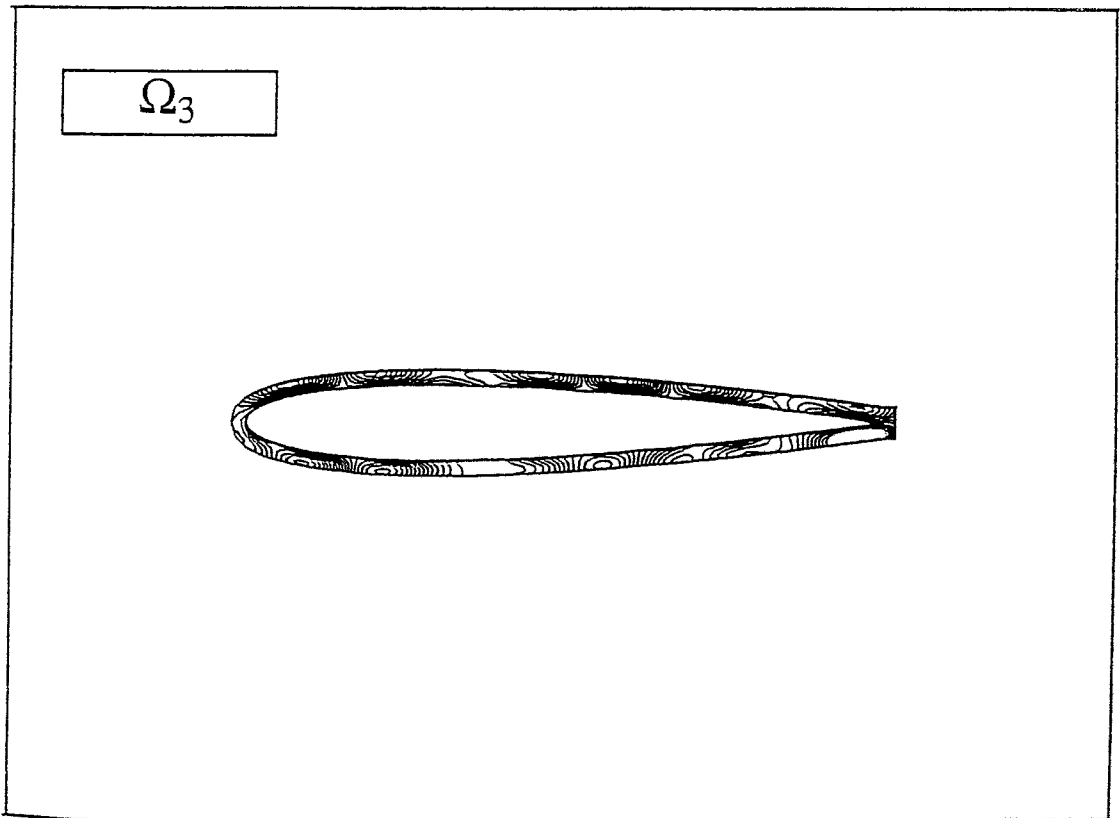


Figure 8.4

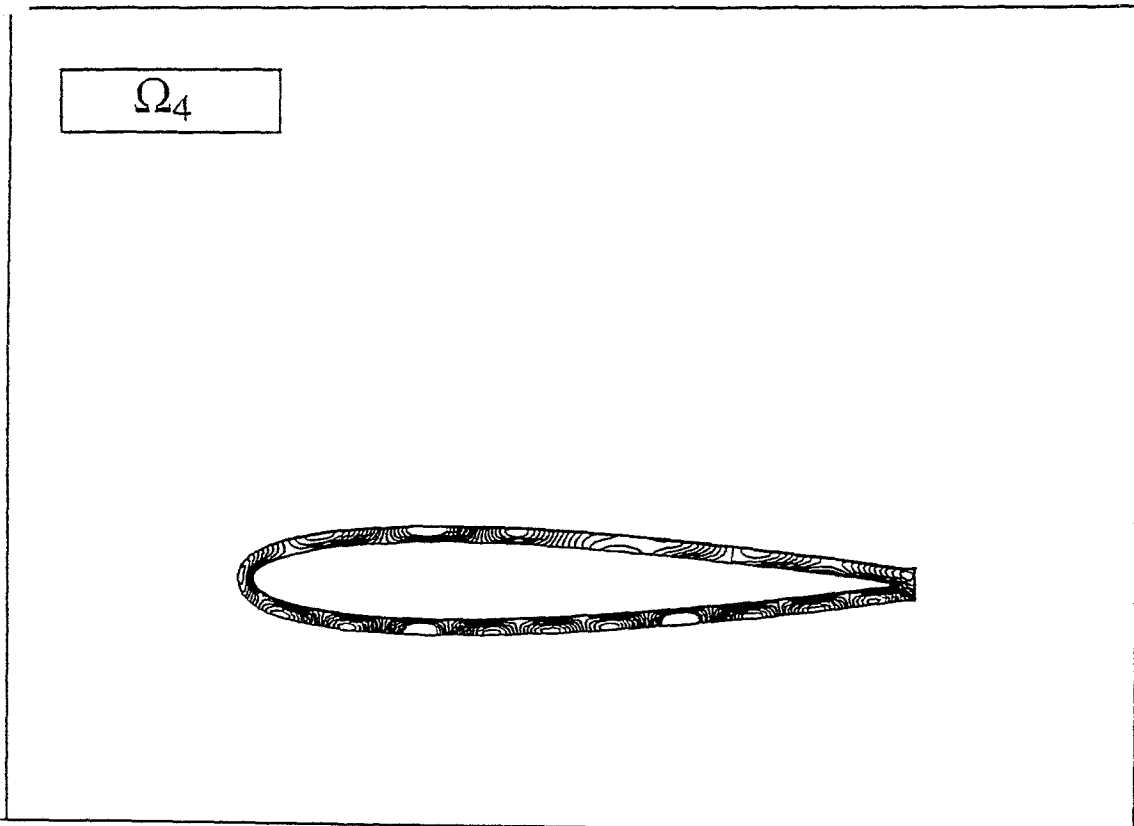


Figure 8.5

Acknowledgments.

The authors would like to thank A. Bamberger, Ch. de la Foye, F. El Dabaghi, P. Joly, A. Lanusse, P. Le Tallec, J. L. Lions, P. Perrier, A. Priou, H. Steve, and Q. H. Tran for helpful comments and suggestions. The supports of DRET (Contract 93.388), IFP, DARPA (Contract AFOSR-90-0334), NSF (Grants INT 86 1268, DMS 8822522, RII 8917691, DMS 9046924, DMS 9408151) and of the Texas Board of Higher Education (Grants 003652156ARP, 003652146ATP, 003652091ARP) are also acknowledged.

References.

- [1] M. O. BRISTEAU, E. J. DEAN, R. GLOWINSKI, V. KWOK, J. PERIAUX, Application of exact controllability to the computation of scattering waves, in *Control Problems in Industry*, I. Lasieka and B. Morton, eds., Birkhäuser, Boston, 1995, pp.17-41.
- [2] J. L. LIONS, Exact controllability, stabilization, and perturbation of distributed systems, *SIAM Review*, (1988), **30**, pp.1-68.
- [3] E. J. DEAN, R. GLOWINSKI, A domain decomposition method for the wave equation, in *Les Grands Systèmes des Sciences et de la Technologie*, J. Horowitz and J. L. Lions, eds., Masson, Paris, 1993, pp.241-264.
- [4] M. O. BRISTEAU, R. GLOWINSKI, J. PERIAUX, Using exact controllability to solve the Helmholtz equation at high wave numbers, Chapter 12 of *Mathematical and Numerical Aspects of Wave Propagation*, R. Kleinman, Th. Angel, D. Colton, F. Santosa, I. Strakgold, eds., SIAM, Philadelphia, 1993, pp.113-127.
- [5] R. GLOWINSKI, J. L. LIONS, Exact and approximate controllability for distributed parameter systems (I), *Acta Numerica*, 1994, pp.269-378.
- [6] R. GLOWINSKI, J. L. LIONS, Exact and approximate controllability for distributed parameter systems (II), *Acta Numerica*, 1995, pp.159-333.
- [7] R. GLOWINSKI, Ensuring well-posedness by analogy: Stokes problem and boundary control for the wave equation, *Journal of Computational Physics*, **103**, (1992), pp.189-221.
- [8] R. GLOWINSKI, M. F. WHEELER, Domain Decomposition and Mixed Finite Element Methods for Elliptic Problems, in *Domain Decomposition Methods for Partial Differential Equations*, R. Glowinski, G. H. Golub, G. Meurant, J. Periaux, eds., SIAM, Philadelphia, 1988, pp.144-172.
- [9] L. C. COWSAR, E. J. DEAN, R. GLOWINSKI, P. LE TALLEC, C. H. LI, J. PERIAUX, M. F. WHEELER, Decomposition principles and their applications in Scientific Computing, in *Parallel Processing for Scientific Computing*, J. Dongarra, K. Kennedy, P. Messina, D. G. Sorensen, R. G. Voigt, eds., SIAM, Philadelphia, 1992, pp.213-237.
- [10] M. FORTIN, R. GLOWINSKI, *Augmented Lagrangians*, North-Holland, Amsterdam, 1983.
- [11] R. GLOWINSKI, P. LE TALLEC, *Augmented Lagrangian and Operator Splitting Methods in Nonlinear Mechanics*, SIAM, Philadelphia, 1989.
- [12] V. KWOK, *Méthodes de Contrôlabilité Exacte et de Décomposition de Domaines*

pour la Résolution Numérique des Equations de l'Electro-Magnétisme en Régime Harmonique dans un Milieu Hétérogène, Ph.D. dissertation, Université P. et M. Curie, Paris, France, July 1995.

Affiliations.

M. O. Bristeau, INRIA, B.16, 78153 Le Chesnay, France. E. J. Dean, University of Houston, Department of Mathematics, Houston, Texas, 77204-3476, USA. R. Glowinski, University of Houston, Department of Mathematics, Houston, Texas, 77204-3476, USA. V. Kwok, Dassault Aviation, 78 Quai Marcel Dassault, 92214 Saint Cloud, France. J. Periaux, Dassault Aviation, 78 Quai Marcel Dassault, 92214 Saint Cloud, France.